7

ROLE OF VASOACTIVE INTESTINAL PEPTIDE IN THE LIGHT INPUT TO THE CIRCADIAN SYSTEM

Andrew Vosko, Hester C. van Diepen, Dika Kuljis, Andrew M. Chiu, Djai Heyer, Huub Terra, Ellen Carpenter, Stephan Michel, Johanna H. Meijer, Christopher S. Colwell

Published in European Journal of Neuroscience 2015, Epub 2015 Apr 17

ABSTRACT

The neuropeptide vasoactive intestinal peptide is expressed at high levels in a subset of neurons in ventral region of the suprachiasmatic nucleus (SCN). While VIP is known to be important for the synchronization of the SCN network, the role of VIP in photic regulation of the circadian system has received less attention. In the present study, we found that the light-evoked increase in electrical activity *in vi*vo was unaltered by the loss of VIP. In the absence of VIP, the ventral SCN still exhibited NMDA-evoked responses in a brain slice preparation although the absolute levels of neural activity before and after treatment were significantly reduced. Next, we used calcium imaging techniques to determine if the loss of VIP altered the calcium influx due to retinohypothalamic tract stimulation. The magnitude of the evoked calcium influx was not reduced in the ventral SCN but did decline in the dorsal SCN regions. We examined the time course of the photic induction of *Period1* in the SCN using *in situ* hybridization in VIP-mutant mice. We found that the initial induction of *Period1* was not reduced by the loss of this signaling peptide. However, the sustained increase in *Period1* expression (after 30 min) was significantly reduced. Similar results were found by measuring the light-induction of cFOS in the SCN. These findings suggest that VIP is critical for longer term changes within the SCN circuit but does not play a role in the acute light response.

INTRODUCTION

Daily biological rhythms are intrinsically generated, synchronized, and regulated by networks of circadian oscillators. These oscillations are generated by robust negative feedback mechanisms that occur at the molecular, cytoplasmic, and membrane levels within single cells [1, 2]. In mammals, the suprachiasmatic nucleus (SCN) of the hypothalamus contains the master oscillatory neurons necessary for coordinating these rhythms found throughout the body [3, 4]. These SCN pacemaker neurons receive integrate timing cues such as daylight and food availability to adjust their rhythmic output [5]. The SCN is divided into core and shell regions [6]: the dorsally-situated shell region contains the majority of the endogenously oscillating neurons in the nucleus, and the ventral core region receives afferent sensory signals [7].

Light is the most powerful environmental cue to which circadian rhythms synchronize [8, 9]. Photic cues are detected by specialized intrinsically photosensitive retinal ganglion cells (pRGCs) containing the photopigment melanopsin [10-12]. The axons of pRGCs form the retinohypothalamic tract (RHT) which terminates on the ventral aspect of the SCN [13-15]. RHT terminals release glutamate and, under certain conditions, the neuropeptide PACAP [16, 17] with the result of photic stimulation being the increase in firing rate of SCN neurons [18, 19]. In SCN neurons, N-Methyl-D-aspartic acid (NMDA) receptor activation and increases in intracellular calcium (Ca^{2+}; [20, 21] play a special role in mediating the effects of RHT activity. The influx of Ca^{2+} in retinally innervated SCN neurons triggers a number of signal transduction pathways that promote the transcription of a set of genes through CREB phosphorylation including the clock gene *Per1* [7, 22, 23] and the immediate early gene cFOS [24]. These molecular light evoked changes in gene expression are thought to be necessary to cause light-induced phase shifts in physiology and behavior [25].

Although the detailed mechanisms by which the SCN circuit operates remains unknown, a major role for vasoactive intestinal peptide (VIP) in photic resetting is indicated. Behaviorally, VIP-deficient mice show clear deficits in their circadian light response [26] and our hypothesis was that the light-evoked changes in SCN physiology would also be compromised. Therefore, in the present study, we first examined the SCN response to light *in vivo* using MUA recordings of freely-moving VIP KO mice and littermate wild-type (WT) controls. We then measured NMDA-evoked responses in ventral SCN neurons in a brain slice preparation of both genotypes. Next, Fura2 calcium imaging techniques were used to measure the calcium transients evoked by electrical stimulation of the RHT *in vitro*. Digoxigenin *in situ* hybridization (ISH) was used to follow the light-induction of *Per1* message in the SCN of both genotypes. Light induction of cFOS in the SCN was examined with immunohistochemical (IHC) techniques.

MATERIALS AND METHODS

Animals

Experimental protocols used in this study were approved by the University of California, Los Angeles or Leiden University Animal Research Committee. Recommendations for animal use and welfare, as dictated by the UCLA Division of Laboratory Animals and the guidelines from the National Institutes of Health, were followed. Adult male (1.5-5 months) WT C57Bl/6 mice and mice lacking the gene encoding for the neuropeptides VIP (VIP KO)[26] were obtained from a breeding facility at the University of California, Los Angeles or from the breeding facility at Leiden University. Mice were group housed until they were used for experiments. Total of 102 C57 mice were used with half being the VIP KO.

In vivo SCN recordings

Mice were implanted with a tripolar stainless steel micro electrode (Plastics One, Roanoke, VA USA) using a stereotaxic instrument (Stoelting, Wood Dale, IL, USA) as previously described [27, 28]. Two polyimide-insulated and twisted electrodes were aimed at the SCN and a third uncoated electrode was placed in the cortex as a reference. Mice were anaesthetized using a mix of ketamine (100mg/kg), xylaxine (20mg/kg) and atropine (1mg/kg). The electrodes were implanted under a 5˚ angle at the same rostrocaudal level as bregma, 0.61 mm lateral to midline and 5.38 mm ventral to the dura mater. The electrode was fixed to the skull using three screws and dental cement. After a week of recovery animals were placed in a custom designed recording chamber to measure SCN electrical activity and behavioral activity using passive infrared sensors simultaneously. Animals were connected to the recording system using a counterbalanced swivel system in which they were able to freely move. The electrical signal was amplified and bandwidth filtered (0.5-5kHz). Window discriminators were used to convert action potentials into digital pulses that were counted in 2 sec epochs.

Animals were recorded over at least two days in continuous darkness. After two days of continuous darkness animals were exposed to 5 minutes of light (fluorescent light source; 150 μW/cm2) at CT 14-16 (2-7 pulses). The circadian time of the light response was calculated per day on the basis of the onset of behavioral activity recorded by a passive infrared sensor in the recording chamber. For quantification of the response, the increases in SCN electrical activity were compared to baseline levels. Baseline levels were defined as 50 sec before lights on and the level of sustained light-induced increase was defined as the average firing rate during lights on (>5 sec after light onset). At the end of each recording, animals were sacrificed and brain tissue was collected for histological verification of the electrode location. After brain fixation in a 4% paraformaldehyde solution containing ferrocyanide, brains were sectioned coronally and stained with cresyl violet. The position of the

electrode was determined by microscopic inspection. Electrodes outside the SCN were excluded from analysis.

Whole cell patch clamp electrophysiology

Mid-SCN coronal slices were collected with a vibratome in slice solution (in mM: 26 $NaHCO_3$, 1.25 NaH_2PO_4, 10 glucose, 125 NaCl, 3 KCl, 5 $MgCl_2$, 1 $CaCl_2$) from Per2::luciferase (P2L) mice and VIP KO x P2L littermates between 1.5 and 3 months of age. Slices were attached to the stage of a fixed-stage upright DIC microscope (Olympus, Tokyo, Japan), and superfused continuously with aerated (95% O_2/5%CO_2) artificial cerebrospinal fluid (ACSF in mM: 26 $NaHCO_3$, 1.25 NaH_2PO_4, 10 glucose, 125 NaCl, 3 KCl, 2 $MgCl_2$, 2 $CaCl_2$). Recording electrodes (4-8MΩ) were pulled from glass capillaries (WPI, Sarasota, FL) on a multistage puller (Sutter P97, Novato, CA, USA) and recording electrodes were filled with standard internal solution (in mM): K-gluconate, 112.5; EGTA, 1; Hepes, 10; MgATP, 5; GTP, 1; leupeptin, 0.1; phosphocreatine, 10; NaCl, 4; KCl, 17.5; $CaCl_2$, 0.5; and $MgCl_2$, 1. Recordings were obtained using the AXOPATCH 200B amplifier (Molecular Devices, Sunnyvale, CA, USA) and monitored on-line with pCLAMP (Ver. 10, Molecular Devices). Each cell was visualized to be within the SCN by means of DIC microscopy, with ventral cells specifically being in close proximity to the optic chiasm. After forming a high resistance seal (>1 GΩ), a second pulse of negative pressure was used to break the membrane. In voltage clamp configuration, most cells had a capacitance between 6 and 15pF, and cells with access resistance higher than 60 MΩ or holding currents larger than -30 pA (at V_{Hold} = -70 mV) were excluded from additional analysis. Junction potential between the pipette and extracellular solution was cancelled by voltage offset of the amplifier before establishing a seal. All solutions' pH was adjusted to 7.25-7.3 and osmolarity adjusted to 290-300 mOsm.

Spontaneous firing rates (SFR) were recorded using current-clamp in the whole cell patch configuration. N-methyl-D-aspartate (NMDA; 25μM) was applied for at least 2 minutes before neuronal SFR was recorded. Following NMDA treatment, ACSF was used to wash slices and determine whether cells were able to re-hyperpolarize following pharmacological excitation to insure healthy cells were selected for analysis. All recording were made in presence of the $GABA_A$ receptor blocker gabazine (10μM; Tocris, Minneapolis, MN, USA). Chemicals were purchased from Sigma-Aldrich (St. Louis, MO, USA) unless otherwise noted.

In vitro calcium (Ca^{2+}) imaging

Brain slices containing the SCN were collected as described above from animals 6-10 weeks of age and loaded with the ratiometric Ca2+ indicator dye fura-2-acetoxymethyl ester (Fura-2-AM, Teflabs, Austin, TX, USA) as previously described [29]. A monochromator (Polychrome V, TILL Photonics, Gräfeling, Germany) was used to deliver paired 50 ms light pulses of two excitation wavelengths (340 and

380 nM). Emitted light (505 nM) was detected by a cooled CCD camera (Sensicam, TILL Photonics), and images were acquired at 2s intervals (0.5 Hz). Single-wavelength images were background subtracted, and ratio images (340/380) generated. Cells were defined as ventral or dorsal based on proximity to the optic chiasm or third ventricle respectively, and the mean ratio values for these region-of-interest-defined cells were used to calculate intracellular Ca2+ concentration. Experiments were conducted using imaging software TILLvisION (TILL Photonics).

For electrical stimulation of the retinohypothalamic tract (RHT) a concentric bipolar electrode (125 µm/Rnd/ 25 µm Pt-Ir, purchased from FHC, Bowdoin, ME, USA) connected to a a Grass S88 Stimulator (Warwick, RI, USA) was placed in the center of the optic chiasm of a coronal hypothalamic slice. The stimulation strength was adjusted to elicit clear Ca^{2+} transient with a fast recovery to baseline levels. The cells were stimulated at 10 Hz for one sec with pulse duration of 200 µs. This train of stimuli was repeated three times with a 60 sec pause between stimulations.

Data were collected and analyzed using Tillvision, Igor Pro (Wavemetrics, Portland, OR), Excel (Microsoft, Redmond, WA), and SPSS 20 (IBM, Armonk, NY). First, baseline Ca^{2+} concentration were examined using mean and SD of signal 14 seconds before each peak in every cell. Cells with a baseline $[Ca^{2+}]_i$ larger than 600 mM were excluded from the data set. Peak Ca^{2+} responses of the remaining cells were included if they exceeded the fluctuations in baseline (larger than two-time the SD) for at least two of the three repeats of the stimulation. The remaining Ca^{2+} responses were also visually checked for abnormalities like steep rise in baseline and erratic Ca^{2+} spikes. Finally, using SPSS software, outliers were identified and removed from the dataset.

Digoxigenin in situ hybridization (ISH)

A plasmid (pCRII; Invitrogen, Carlsbad, CA, USA) containing the cDNA for Per1 (340– 761 nucleotides, accession number AF022992) was generously provided by Dr. D. Weaver (University of Massachusetts), and insert identity was confirmed by sequencing using the M13R primer. To generate antisense and sense templates for hybridization, plasmids were linearized overnight, phenol-chloroform extracted, ethanol precipitated and re-suspended in diethyl pyrocarbonate (DEPC)-treated water.

Digoxigenin-labeled riboprobes were generated from 1 µg of template cDNA in a reaction mixture containing 2 µl of 10X concentrated digoxigenin (DIG) RNA Labeling Mix (Roche Applied Science Indianapolis, IN, USA), 2 µl of 10X concentrated Transcription Buffer (Roche Applied Science, Indianapolis, IN, USA), 40 U Rnase Block (Stratagene, La Jolla, CA, USA), and 2 µl of the appropriate RNA transcriptase (SP6, or T7; Roche Applied Science, Indianapolis, IN, USA) for 2 hours at 37°C. The in vitro transcription reaction was terminated by the addition of 2 µl of 0.2 M EDTA and precipitated with 2.5 µl of 4 M LiCl and 100% ethanol overnight at -20°C.

Precipitate was extracted with 70% ethanol and reconstituted in 100 µl of sterile water. Probe yield estimates were determined using relative densities of known concentrations of untranscribed, linearized plasmid in gel electrophoresis and also from serial dilutions of cross-linked riboprobe bound to alkaline phosphatase-conjugated anti-DIG antibody (Roche Applied Science, Indianapolis, IN, USA) visualized with 4-Nitro blue tetrazolium (NBT) and 5-Bromo-4-chloro-3-indolyl phosphate (BCIP) (Roche Applied Science, Indianapolis, IN, USA).

Prior to brain collection, wheel running activity was measured as described previously (Loh et al., 2013). Male VIP-deficient mice were housed in cages containing running wheels (Mini Mitter Co., Bend, OR) from 6-7 weeks of age and their wheel-running activity recorded as revolutions (rev) per 3 min intervals. Animals were exposed to a 12:12 hr light-dark cycle (LD; light intensity 350 lux) for 10 days, and then released to 24 hr of constant darkness (DD) to assess their free-running activity pattern for 7-10 days. Animals were given a 10 minute light pulse (light intensity ≈ 50 lux) at circadian time (CT) 16 based on wheel running activity records (CT 12 was defined as activity onset) and sacrificed after either 30, 60, 90, or 120 minutes under anesthesia (n=3-5 in each condition). Control animals were culled at the same time without a light pulse. Brains were removed, flash-frozen, sectioned at 20 µM and slide mounted, then stored at -80°C until hybridization or immunofluorescence.

On the first day of hybridization, slides were warmed to room temperature and fixed in 4% paraformaldehyde. Following brief washes in PBS, slides were placed in prehybridization buffer (50% formamide, 5X SSC, 1% SDS, 0.2% Tween-20, 0.1% heparin, and 50 ng/mL Torula RNA) at 60°C for 1- 2 hours. Sections were then hybridized overnight at 60°C in hybridization buffer (50% formamide, 5X SSC, 1% SDS, 0.2% Tween-20, 0.1% heparin, and 50 ng/mL Torula RNA), and ≈ 50-100 pg/µL of riboprobe) in sealed slide mailers. Following hybridization, slides were washed briefly in 5X SSC and then for 1 hour in 0.2X SSC at 60°C to remove unbound probe. Slides were then briefly washed with maleic acid buffer (0.1M maleic acid, 0.15M NaCl) and blocked in 20% heat-treated sheep serum in maleic acid buffer. After blocking, slides were incubated with 1:500 anti-DIG antibody conjugated to alkaline phosphatase (Roche Applied Science, Indianapolis, IN, USA) in a humid chamber at 4°C overnight. After antibody incubation, slides were washed in maleic acid buffer and then in tris buffer (0.1 M Tris (pH 9.5), 0.1 M NaCl, and 5 mM MgCl2). For revelation, slides were incubated in a color reaction solution (tris buffer, 0.3375% NBT, 0.35% BCIP, 1mM levimasole) at room temperature overnight in a humid chamber. After revelation, slides were washed with PBS and color was preserved via a final incubation in 4% paraformaldehyde containing EDTA. Slides were then cover-slipped and imaged on an Olympus microscope using Axiovision software (Carl Zeiss Inc., Thornwood, NY) for analysis. Sense probe hybridization showed no positive staining.

For quantification, SCN sections were imaged and SCN borders were determined by 4',6- Diamidino-2-Phenylindole, Dihydrochloride (DAPI) and arginine vasopressin (AVP) distribution dorsal to the optic chiasm in the anterior hypothalamus. For each SCN, a template was created to define core and shell subregions delineated by AVP expression. This delineation was confirmed by additionally double immunostaining against AR to confirm that a lack of AVP signal coincided with the SCN core. Templates from adjacent sections were superimposed onto both Per1+ and c-FOS+ sections and the resulting mid-SCN image (unilateral) for each animal was counted by an experimenter blind to condition.

Immunohistochemistry (IHC)

Brains were processed as described above, and alternate sections were used to delineate SCN subregions chemo-architecturally. Sections were fixed in 4% paraformaldehyde at room temperature, washed with PBS, and incubated in blocking solution (3% normal goat serum (NGS), 0.1% Triton X-100 in PBS). After blocking, sections were incubated with a guinea pig polyclonal antibody raised against arginine-vasopressin (AVP, 1:000; Bachem, Torrance, CA); a rabbit polyclonal antibody raised against FOS (1:30,000; Merck Millipore, Darmstadt, Germany); or a rabbit polyclonal antibody raised against androgen receptor (AR; 1:150; Santa Cruz Biotechnology, Santa Cruz, CA) in blocking solution at 4°C for 4 days. Sections were then washed and incubated with Alexa Fluor® 568-conjugated goat anti-guinea pig IgG antisera (Molecular Probes, Eugene, OR), diluted to 1:300 with blocking solution at room temperature. If tissue was processed for double immunostaining, primary antibody incubation was carried out with both the primary AVP antibody and a rabbit polyclonal antibody raised against androgen receptor (AR) (Santa Cruz Biotechnology, Santa Cruz, CA) diluted at 1:150. Also, during the secondary antibody incubation, Alexo Fluor® 488-conjugated secondary antisera (Molecular Probes, Eugene, OR), diluted at 1:200, was additionally used. After incubation with secondary antibody, sections were again washed with PBS, cover slipped with Vectashield Mounting Media containing DAPI (Vector Laboratories, Burlingame, CA), and stored in the dark at 4°C until imaged.

Statistical measurements

The data sets were analyzed for equal variance and normal distribution to help select the appropriate statistical test. Significance for electrophysiological recordings and Ca^{2+} imaging was assessed using a Student's *t*-test as well as two-way analysis of variance (ANOVA), with genotype and light or NMDA exposure as factors. Paired Student's *t*-tests were used to detect significant changes due to pharmacological treatment and unpaired Student's *t*-tests were used to assess differences in spontaneous electrical activity due to genotype. Effects were reported to be significant if $P < 0.05$. For ISH, the data sets were analyzed by two-way ANOVA,

with genotype and light exposure as factors. If significant group differences were detected ($P < 0.05$) by ANOVA, then the Holm–Sidak method for pair-wise multiple comparisons was used. For all tests, values were considered significantly different if $P < 0.05$. All tests were performed using Sigmastat software (version 3.5, Systat Software, San Jose, CA, USA). Values are shown as mean ± SEM.

RESULTS

In vivo electrophysiology finds no deficits in light evoked responses in SCN of VIP mutants

Using *in vivo* extracellular recording techniques, SCN electrical activity was measured in both VIP KO (n=7) and WT controls (n=5). Physiological responses were used to confirm that the electrode was placed in a light-response region of the SCN and histological analysis confirmed that each of these recordings was made in the SCN. Successful recordings showed high SCN electrical activity during the day and low electrical activity during the night. Light exposure induced an increase in the SCN electrical discharge pattern with a transient overshoot at lights on and a sustained elevation in SCN electrical activity throughout light exposure (Fig. 1A). No differences in light response characteristics were detected between VIP KO and WT mice (KO: 12 ± 2 % change; WT: 16 ± 6 %; *t*-test: $P > 0.05$; Fig. 1B). Both genotypes showed a significant increase in SCN electrical activity upon light exposure during the night (CT 14-16) (Fig. 1C). Two-way ANOVA (DF =23) was also performed to test for genotype and treatment effects. Main effect of light treatment (F=15.610, P=0.003) was identified, but no effect of genotype (F=0.173, P=0.687). These results demonstrate that photic information is reaching the retino-recipient cells in the SCN in the VIP KO mice.

In vitro electrophysiology demonstrates reduced baseline activity but robust NMDA-evoked changes in ventral SCN neurons

A variety of evidence suggests that the effects of light on the mammalian circadian system are mediated by glutamatergic mechanisms and that the NMDA receptor plays an important role in this regulation. Using the whole cell patch-clamp recording technique in current clamp mode, we measured the SFR in ventral SCN neurons in a brain slice preparation in response to bath application of NMDA (25μM, 3min). Each of these cells was determined to be within the ventral region of the SCN by directly visualizing the location of the cell as being immediately adjacent to or in close proximity with the optic chiasm using infrared DIC video microscopy. In WT mice, ventral SCN neurons responded to bath application of NMDA with an increase in SFR (Fig. 2, P <0.001). The VIP KO also showed a significant response to NMDA treatment (P = 0.02), but there were differences between the genotypes. First, the absolute SFR was reduced in mutant SCN compared to WT in both baseline (WT: 1.76 ± 0.4 Hz vs. VIP KO: 0.48 ± 0.2 Hz,

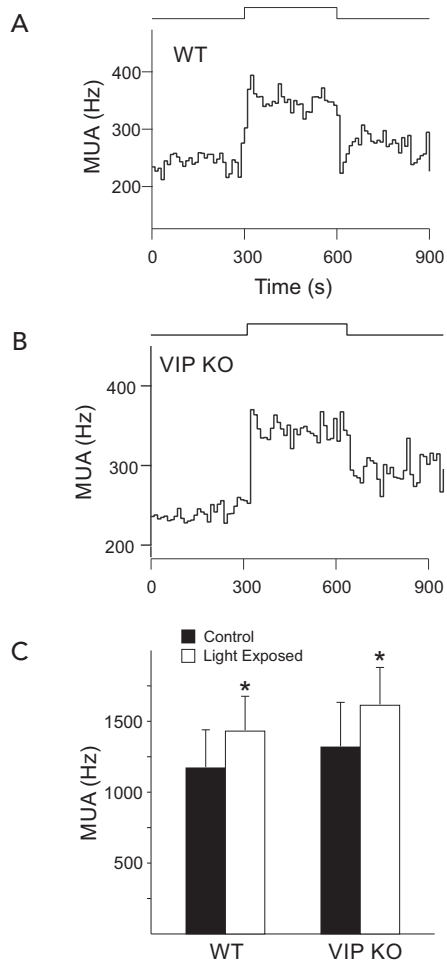

Figure 1. Light-evoked changes in multiunit activity (MUA) recorded from the SCN of freely moving mice. (A, B) Representative examples of MUA rhythms recorded from the SCN of a WT and VIP KO mouse during the night. Light pulses are indicated above the graphs. SCN firing rate is increased in both VIP KO and WT mice, with a response latency of 0.04 sec. Bin size is 0.01 sec. (C) bar graphs show mean and SEM of the MUA before and during light exposure. * indicates significant difference ($P<0.05$) compared to controls analyzed by two-way ANOVA followed by Holm-Sidak method for multiple comparisons. There were no differences between the two genotypes.

P =0.03) and NMDA treatment conditions (WT: 4.11 ± 1.0 Hz vs. VIP KO: 1.44 ± 0.4 Hz, P = 0.04). Second, whereas all WT neurons (16/16) responded to NMDA treatment with increased firing rates, only 9 out of 13 mutant neurons did (Chi2 = 5.7; P=0.008). Two-way ANOVA (DF=57) was also performed to test for genotype and treatment effects. Main effects of genotype (F=9.59, P=0.003)

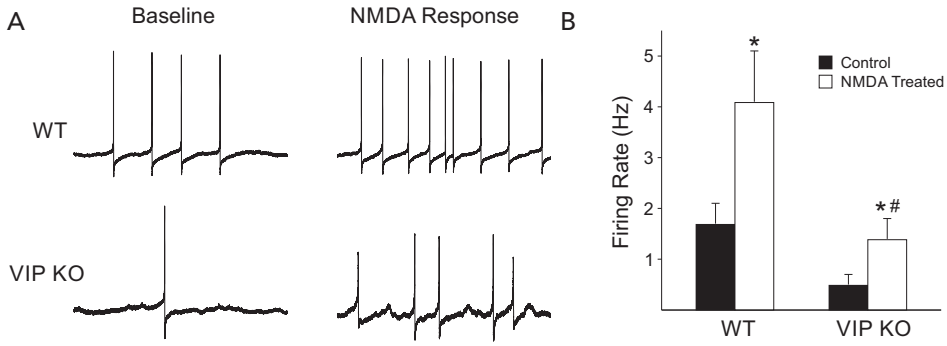

Figure 2. Application of NMDA increased the firing rate of ventral SCN neurons during the night *in vitro*. (A) Representative examples illustrating the NMDA-induced increase in firing rate in a ventral SCN neuron from the VIP KO and WT control mice. (B) Bar graphs show average firing rate for each group (SEM). * indicates significant difference ($P<0.05$) compared to controls analyzed by two-way ANOVA followed by Holm-Sidak method for multiple comparisons. # indicates a significant difference between the two genotypes.

and NMDA treatment ($F=8.17$, $P= 0.006$) were identified, but no interaction of genotype and treatment ($F=1.20$, $P=0.279$). Thus, in the ventral SCN region, while the absolute levels of neural activity were reduced in VIP deficient mice, NMDA still evoked a significant change in firing of these neurons although the excitatory effects were less uniform than in WT.

Ca^{2+} imaging indicates RHT stimulation normal in ventral SCN cell population but reveals deficits in dorsal SCN in VIP KO mice.

Release of glutamate from RHT terminals in the SCN after electrical stimulation will lead to an increase in intracellular Ca^{2+} (Irwin & Allen, 2007) and ultimately phase shifts of the circadian system. Optical imaging techniques and fura2-AM indicator dye were used to measure RHT-stimulated Ca^{2+} transients in SCN cells in the night. RHT stimulation produced a reliable increase in $[Ca^{2+}]_i$ in a subset of SCN neurons in both ventral (WT: 40%; KO: 38%) and dorsal (WT: 20%; KO: 19%) cell populations (S. Fig. 1). In the ventral SCN region, the magnitude of the RHT-evoked Ca^{2+} transient was enhanced in the VIP-deficient mice (Fig. 3A), while in the dorsal SCN, there was a 30% reduction in the amplitude of RHT-evoked Ca^{2+} increases (Fig. 3B). The baseline in Ca^{2+} levels measured during the night were low and did not vary between the genotypes (Fig. 3C). Two-way ANOVA ($DF=580$) indicated no main effect of the Ca^{2+} increases, but there were significant effects of region ($F=50.860$, $P=0.001$) and a significant interaction between genotype x region ($F=9.473$, $P=0.002$) Thus, as measured by Ca^{2+} transients, the ventral SCN cell population appears to be receiving the signal from the RHT but the dorsal SCN cells exhibit a weakened response in the absence of VIP.

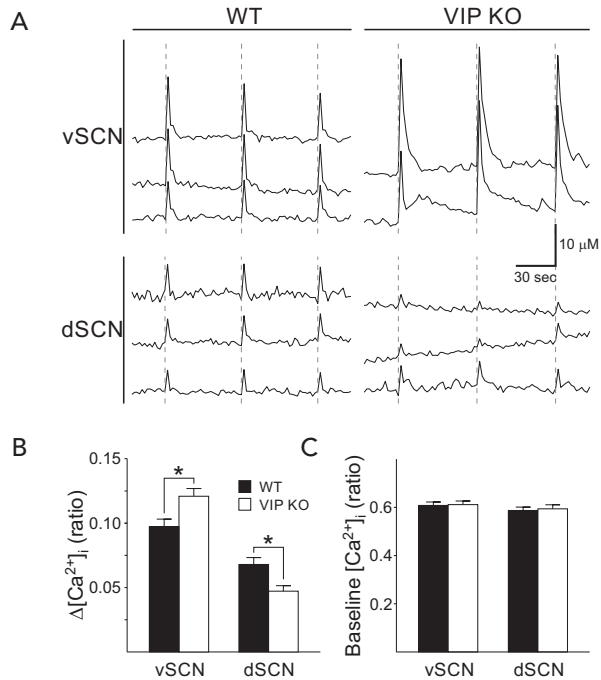

Figure 3. Evoked Ca^{2+} transients in the SCN of VIP KO and WT controls in response to RHT stimulation in a brain slice. (A) Examples of increases in $[Ca^{2+}]_i$ after electrical stimulation of the RHT (dotted line; 10Hz for 1 sec) in the ventral and dorsal region of the SCN for both WT and VIP KO mice. Each line represents the response of one cell to three repeated stimuli. (B) Average change in $[Ca^{2+}]_i$ expressed in ratio (340 nm/380 nm) after RHT stimulation. Compared to WT controls, the VIP KO mice show higher responses in the ventral SCN (P = 0.005), but lower responses in the dorsal SCN (P = 0.003) after RHT stimulation. Error bars represent SEM. * indicates significant difference (P<0.01) compared to controls analyzed by two-way ANOVA followed by Holm-Sidak method for multiple comparisons. (C) Average baseline $[Ca^{2+}]_i$ does not differ between the genotypes, nor between ventral and dorsal SCN.

7

The loss of VIP alters the temporal and spatial distribution of light-evoked increases in Period1 expression in the SCN.

To establish how light-induced *Per1* expression varied between the genotypes, digoxigenin *in situ* hybridization on SCN tissue at 30, 60, 120 min after light exposure at CT 16 (50 lux, 10 min) was performed. SCN photomicrographs illustrate that WT and VIP deficient mice differ in the spatio-temporal expression profiles of *Per1* (Fig. 4, 5). As has been previously reported (Yan and Silver, 2004) in WT SCN, *Per1* is photically induced in two separate waves: one in the core followed by one in the shell. The majority of immediate light-induced *Per1* expression occurs during the first wave in the SCN core. This is followed by a second wave in the shell, characterized by a steady increase of *Per1* from 30 to 90 min. In VIP

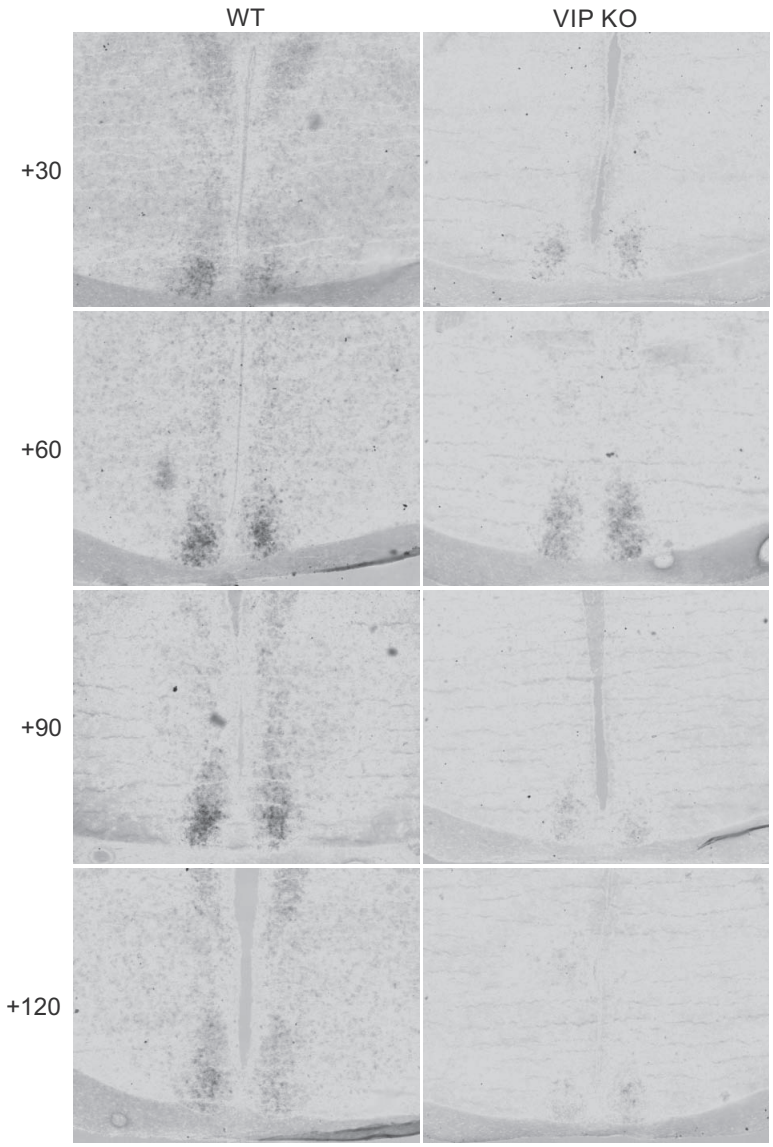

Figure 4. Examples of the temporal pattern of light-evoked changes in *Per1* mRNA. SCN photomicrographs following digoxigenin ISH for *Per1* reveal a time course of induction in WT mice at CT 16. Message begins to appear around 30 min after the beginning of the light pulse, with well-defined expression in a subpopulation of cells in the ventro-middle region of the nucleus around 45 to 60 min after the initial pulse. Message expression spreads across the nucleus and disappears by 4 hours after the initial pulse. This pattern is disrupted in the VIP KO mice in which the initial induction of the *Per1* in response to light is strong but the signal is not sustained nor communicated to the shell SCN region. Upper left panel is labeled with PVN (paraventricular nucleus), SCN (suprachiasmatic nucleus), OC (optic chiasm), and 3rd V (3rd ventricle) as an aid for the reader.

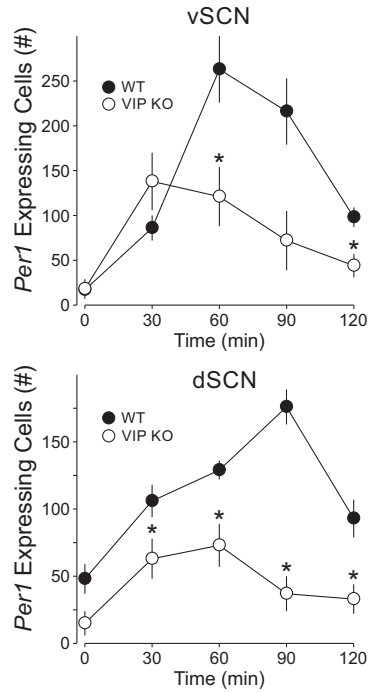

Figure 5. Quantification of the temporal patterns of light-evoked *Per1* expression in the core and shell SCN. Cell counting of *Per1*+ cells following ISH reveals that*Per1* is significantly induced by a CT 16 light pulse at all-time points measured in WT mice, but only at 30 and 60 min post pulse in VIP KO mice. Post hoc analyses reveal significantly reduced *Per1*+ cell counts in the VIP KO compared with controls at 30, 60, and 90 min time points in the core SCN (denoted by *). In the shell, all *Per1*+ cell counts were significantly reduced. * indicates significant difference ($P<0.05$) compared to controls analyzed by two-way ANOVA followed by Holm-Sidak method for multiple comparisons.

KO mice, the two waves of *Per1* induction follow a different pattern. Although there was an immediate response to the light pulse with a sizable induction of *Per1* 30 min after the initial light exposure in the SCN core, this first wave of *Per1* induction decreased faster in the VIPKO, at least an hour earlier when compared to WT. Next, the second wave of *Per1* induction in the SCN shell was markedly attenuated in VIPKO mice. In fact, *Per1* levels were similar to untreated controls, although there was some animal to animal variation in mutants. Two-way ANOVA analysis ($DF=38$) of the *Per1* expression in the core revealed effects of genotype ($F=50.216$, $P=0.001$), light treatment ($F=9.272$, $P=0.001$) and interaction of genotype x light treatment ($F=4.109$, $P=0.009$) on light-induced *Per1* expression levels in the mouse SCN.

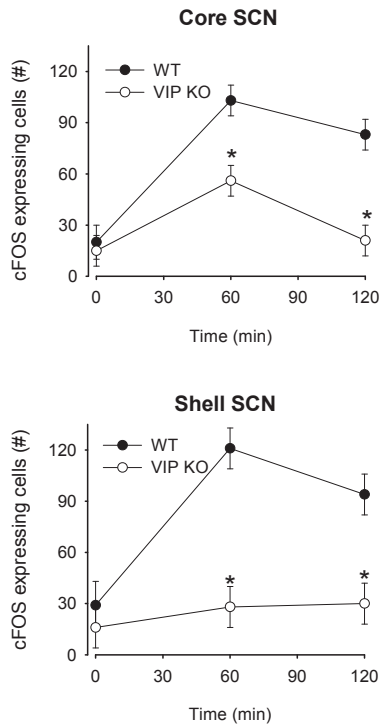

Figure 6. Quantification of the temporal patterns of light-evoked c-FOS expression core and shell SCN. Cell counting of c-FOS+ cells in the SCN core following immunofluorescence reveals that c-FOS is significantly induced by a CT 16 light pulse at both 60 and 120 min following light exposure in WT mice, but only at 60 min post pulse in VIP KO mice. In the SCN shell, c-FOS is significantly induced at both 60 and 120 min following light exposure in the WT mice. There was no significant c-FOS induction in the SCN shell of the mutant mice. *Post hoc* analyses reveal significantly reduced c-FOS+ cell counts in VIP KO mice compared with controls at both the 60 and 120 min time points. * indicates significant difference ($P<0.01$) compared to controls analyzed by two-way ANOVA followed by Holm-Sidak method for multiple comparisons.

We also examined light induction of FOS in the core and shell SCN (Fig. 6). Compared to untreated controls, WT SCN exhibited a significant FOS induction when measured 60 and 120 min after light exposure (50 lux, 10 min) in both the core and shell regions. In contrast, the VIP KO mice only exhibited a significant FOS induction when measured 60 min after light exposure in the core SCN. By 120 min, the FOS counts were back at baseline in the core and never increased in the shell region. Two-way ANOVA analysis ($DF=22$) of FOS expressions in the core revealed effects of genotype ($F=24.851$, $P=0.001$) light treatment ($F=21.776$, $P=0.02$) on light-induced FOS expressions levels in the mouse SCN. Thus in the

VIP KO mice, the light-induction of cFOS and *Per1* are attenuated in duration and most significantly impacted in the shell region of the SCN.

DISCUSSION

Previous studies have provided evidence that VIP signaling is important for synchronization of the circadian oscillator to the environment. Behavioral pharmacology studies have shown that the application of VIP alone [30] or in combination with other peptides [31] can mimic the phase shifting effects of light. In a brain slice preparation containing the SCN, application of VIP induces clock gene expression [32] as well as phase shifts the circadian rhythm of vasopressin release [33] and neural activity [34]. Behaviorally, the loss of VIP signaling alters the synchronization of circadian system. This phenotype is best seen in the experiments in which VIP or VIPR2 KO animals are released into DD from an LD cycle. A normally entrained animal will start its activity from a phase predicted from the prior LD cycle. For example, WT mice begin their free-running rhythm within 30 min of the time of lights-off in the prior LD cycle. In contrast, the VIP KO animals start their activity about 8 to 10 hours before the time of the prior lights-off [26, 35, 36]. Similarly, the VIPR2 KO mice also exhibit an extremely large advance in activity onset after release into DD [37]. This altered synchronization in the VIP KO mice is also seen when the mice are held in a skeleton photoperiod consisting of one or two light exposures per 24 hrs cycle and in the failure of these mice to response to short light exposure with phase shift in their locomotor activity rhythms [26]. The VIP KO mice fail to show behavioral and physiological adaptations to short or long photoperiods [28]. Thus, the data are consistent with the suggestion that VIP is required for normal light-induced synchronization of the circadian system but does not tell us where in the circadian circuit the deficits lie.

To examine this issue, we first implanted electrodes into the SCN of VIP KO mice and litter-mate WT controls and recorded SCN electrical activity in freely moving mice. In response to retinal illumination, light-responsive SCN neurons show an increase in electrical impulse frequency [19, 27, 38-40]. We found that the VIP KO mice exhibited robust light-responses that could not be distinguished from those recorded from the SCN of WT mice (Fig. 1). All of the cells were light-responsive but the nature of these extracellular recording makes it difficult to determine the region of the SCN from which the neurons were sampled. Prior work has established that the RHT mostly terminates on the ventral aspect of the SCN [13-15] and we assume that this is where the greatest % of light-responsive units are located. Given the severe behavioral deficits observed in the photic response of the VIP KO mice, these results were unexpected. These results indicate that the retinal illumination is reaching the SCN of the mutant mice without difficulty.

A variety of evidence indicates that NMDA receptors play a critical role in transducing the glutamatergic RHT signal to an electrical response in the SCN [41-45]. Therefore we next directly measured NMDA-evoked changes in firing rate in SCN neurons in a brain slice preparation. One caveat here is that in order to isolate the NMDA currents, we blocked GABA mediated synaptic transmission which could influence the findings. Focusing on neurons in the retino-recipient ventral region of the SCN, we found that VIP KO and WT mice exhibited clear NMDA-evoked changes in firing rate (Fig. 2). Focusing on neurons in the retino-recipient ventral region of the SCN, we found that VIP KO and WT mice exhibited clear NMDA-evoked changes in firing rate (Fig. 2). This observation fits with the extracellular recording described above. The single cell resolution of the whole cell patch clamp recordings offers a more nuanced view of the impact of the loss of VIP. The absolute level of SCN activity was significantly reduced in the absence of VIP and a smaller percentage of neurons exhibited a significant NMDA-evoked change in firing. These genotypic changes would be very difficult to detect with the extracellular technique used above. So the patch-clamp recording indicate that, while the KO mice exhibit a clear NMDA response, the absolute firing rate with and without NMDA treatments was reduced in the mutant ventral SCN neurons.

After NMDA receptor activation, the next step in the signaling cascade in SCN neurons appears to be an increase in intracellular Ca^{2+} mediated by both glutamate receptor activation as well as depolarization driven activation of voltage sensitive Ca^{2+} channels [20, 21, 46]. Optical imaging techniques and fura2-AM indicator dye were used to measure RHT-stimulated Ca^{2+} transients in SCN cells in the night. While the % of cells responding to RHT did not vary between the genotypes (S. Fig. 4), we saw a striking difference between the ventral and dorsal cell populations. In the ventral SCN region, the RHT-evoked Ca^{2+} transient was actually enhanced in the VIP-deficient mice than in WT (Fig. 3A). This fits with our *in vivo* recordings as shown in Fig. 1. In contrast, in the dorsal SCN region, there was a 30% reduction in the amplitude of RHT-evoked Ca^{2+} increases (Fig. 3B). So the physiological measures indicate that the loss of VIP does not alter the transmission of light-information to the SCN circuit but raise the possibility that the VIP prevents the spread of photic information from the ventral neurons to the rest of the SCN circuit. This hypothesis fits with recent observations suggesting that VIP and its receptor (VIPR2) is necessary for circuit-level integration with the SCN [47, 48].

Finally, we turned to anatomical techniques to further test this model. The increase in Ca^{2+} activates a number of signaling pathways that converge to alter transcriptional and/or translational regulators, including cyclic AMP-responsive element (CRE)-binding protein (CREB). Phosphorylated CREB is translocated into the nucleus where it can bind to CREs in the promoter regions of *c-Fos* and Period1 (*Per1*), and drives transcription of these genes over the course of hours [22, 23, 49-51]. We have previously found that the photic induction of *Per1* in the SCN was

reduced in the VIP KO [52] but did not examine the spatio-temporal patterns in the mutants. So in our final set of experiments, we examined the light-evoked changes in *Per1* and FOS in the SCN of the VIP KO mice. For each SCN, a template was created to define core and shell regions delineated by expression of AVP (shell) and AR (core). As has been previously reported [7, 53] in WT SCN, *Per1* is photically induced in two separate waves: one in the core followed by one in the shell. The majority of immediate light-induced *Per1* expression occurs during the first wave in the SCN core. This is followed by a second wave in the shell, characterized by a steady increase of *Per1* from 30 to 90 min (Fig. 4, 5). The light induction of *Per1* expression in the VIP KO showed a strikingly different pattern. As we have seen with the physiology, the immediate response to the light pulse was a sizable induction of *Per1* 30 min after the initial light exposure in the SCN core VIP KO mice. However, this increase declined faster and the second wave of *Per1* induction in the SCN shell was markedly attenuated in VIP KO mice. As far as we know, this pattern of gene expression has only been reported once before. Mice heterozygous for a mutation in the NaV1.1 channel (*Scn1a* +/−) also show normal light induction of *c-Fos* and *Per1* mRNA in ventral SCN but impaired gene expression responses in dorsal SCN [54]. We do not know the impact of the reduction in the Scn1a gene on SCN electrical activity but a reasonable speculation is that the excitability is reduced in both the *Scn1a* +/- and the VIP KO mice.

Together these findings raise questions about mechanisms and functional significance. The ventral SCN receives most of the retinal input [13-15] and shows more robust light-induced changes in electrical activity [18, 19] and gene expression [55-60]. Many of the neurons that receive retinal input within the core SCN express the neuropeptides vasoactive intestinal protein (VIP) and gastrin-releasing peptide (GRP), as well as the neurotransmitter GABA. In contrast, neurons of the dorsal shell appear to generate the most robust circadian oscillations, at least at the level of gene expression [53, 61, 62]. The neurons in the shell express vasopressin (AVP), prokineticin 2 (PK2) as well as GABA. Therefore VIP is well positioned to mediate core to shell communication. While the VIP receptors (VIPR2) are expressed throughout the SCN, the expression is more abundant in the dorsal region [63] especially in the central SCN where we do our physiological recordings.

Both light exposure as well as treatment with gastrin-releasing peptide (GRP) or VIP can also cause persistent increases in neural activity within the SCN at night [58, 64-66]. Thus peptide transmitters can drive long-lasting changes in the excitability within the SCN network. We speculate that VIP and GRP may work together functionally to regulate the excitability of the SCN circuit. VIP is expressed with a subset of GABAergic interneurons found throughout the central nervous system and has been shown to alter the excitability of several neural populations [67-70]. There is also evidence that SCN neurons from VIPR2-/- mice may be chronically hyperpolarized [71] consistent with the findings in the present study. These findings

suggest that VIP-induced changes in electrical activity may be critical for the light induces changes in gene expression especially in the dorsal SCN. During the night, SCN neurons are normally silent but do respond to photic stimulation transduced by pRGCs that generate action potentials up to 20 Hz [19, 20, 72-74]. This light-induced increase in neural activity drives synaptic communication with the rest of the cells in the circuit. Prior work in both mollusks and mammals suggests that the electrical activity of circadian pacemaker neurons determines how these cells respond to photic stimulation [20, 21, 75]. This regulation can explain why the loss of VIP or its receptor has such a dramatic effect on photic entrainment of the circadian system.

Finally, a study reports that VIP induces rPer1 and rPer2 gene expression during the subjective night [32]. The normal light induction of these Per genes is absent in the Vipr2 -/- mice [37], which also show a lack of phase gating in their response to light [76]. Together, these observations suggest that the VIP/VPAC2R signaling pathway is critical for coupling of the oscillator to the environment. Given the anatomical localization of VIP in the retino-recipient SCN neurons, the simplest explanation is that the loss of VIP prevents the spread of photic information from the ventral neurons to the rest of the SCN circuit and impairs the ability of the SCN to encode seasonal information.

REFERENCES

1. Mohawk, J.A., Green, C.B., and Takahashi, J.S. (2012). Central and peripheral circadian clocks in mammals. Annual review of neuroscience *35*, 445-462.
2. O'Neill, J.S., Maywood, E.S., and Hastings, M.H. (2013). Cellular mechanisms of circadian pacemaking: beyond transcriptional loops. Handbook of experimental pharmacology, 67-103.
3. Dibner, C., Schibler, U., and Albrecht, U. (2010). The mammalian circadian timing system: organization and coordination of central and peripheral clocks. Annual review of physiology *72*, 517-549.
4. Welsh, D.K., Takahashi, J.S., and Kay, S.A. (2010). Suprachiasmatic nucleus: cell autonomy and network properties. Annual review of physiology *72*, 551-577.
5. Challet, E., Caldelas, I., Graff, C., and Pevet, P. (2003). Synchronization of the molecular clockwork by light- and food-related cues in mammals. Biological chemistry *384*, 711-719.
6. Abrahamson, E.E., and Moore, R.Y. (2001). Suprachiasmatic nucleus in the mouse: retinal innervation, intrinsic organization and efferent projections. Brain research *916*, 172-191.
7. Yan, L., and Silver, R. (2004). Resetting the brain clock: time course and localization of mPER1 and mPER2 protein expression in suprachiasmatic nuclei during phase shifts. The European journal of neuroscience *19*, 1105-1109.
8. Czeisler, C.A., Richardson, G.S., Zimmerman, J.C., Moore-Ede, M.C., and Weitzman, E.D. (1981). Entrainment of human circadian rhythms by light-dark cycles: a reassessment. Photochemistry and photobiology *34*, 239-247.
9. Khalsa, S.B., Jewett, M.E., Cajochen, C., and Czeisler, C.A. (2003). A phase response curve to single bright light pulses in human subjects. The Journal of physiology *549*, 945-952.

10. Rollag, M.D., Berson, D.M., and Provencio, I. (2003). Melanopsin, ganglion-cell photoreceptors, and mammalian photoentrainment. Journal of biological rhythms *18*, 227-234.
11. Schmidt, T.M., Do, M.T., Dacey, D., Lucas, R., Hattar, S., and Matynia, A. (2011). Melanopsin-positive intrinsically photosensitive retinal ganglion cells: from form to function. The Journal of neuroscience : the official journal of the Society for Neuroscience *31*, 16094-16101.
12. Lucas, R.J., Lall, G.S., Allen, A.E., and Brown, T.M. (2012). How rod, cone, and melanopsin photoreceptors come together to enlighten the mammalian circadian clock. Progress in brain research *199*, 1-18.
13. Ibata, Y., Takahashi, Y., Okamura, H., Kawakami, F., Terubayashi, H., Kubo, T., and Yanaihara, N. (1989). Vasoactive intestinal peptide (VIP)-like immunoreactive neurons located in the rat suprachiasmatic nucleus receive a direct retinal projection. Neuroscience letters *97*, 1-5.
14. Kiss, J., Csaki, A., Csaba, Z., and Halasz, B. (2008). Synaptic contacts of vesicular glutamate transporter 2 fibres on chemically identified neurons of the hypothalamic suprachiasmatic nucleus of the rat. The European journal of neuroscience *28*, 1760-1774.
15. Morin, L.P., and Allen, C.N. (2006). The circadian visual system, 2005. Brain research reviews *51*, 1-60.
16. Hannibal, J., Brabet, P., and Fahrenkrug, J. (2008). Mice lacking the PACAP type I receptor have impaired photic entrainment and negative masking. American journal of physiology. Regulatory, integrative and comparative physiology *295*, R2050-2058.
17. Hannibal, J., and Fahrenkrug, J. (2002). Melanopsin: a novel photopigment involved in the photoentrainment of the brain's biological clock? Annals of medicine *34*, 401-407.
18. Shibata, S., Liou, S., Ueki, S., and Oomura, Y. (1984). Influence of environmental light-dark cycle and enucleation on activity of suprachiasmatic neurons in slice preparations. Brain research *302*, 75-81.
19. Meijer, J.H., Watanabe, K., Schaap, J., Albus, H., and Detari, L. (1998). Light responsiveness of the suprachiasmatic nucleus: long-term multiunit and single-unit recordings in freely moving rats. The Journal of neuroscience : the official journal of the Society for Neuroscience *18*, 9078-9087.
20. Irwin, R.P., and Allen, C.N. (2007). Calcium response to retinohypothalamic tract synaptic transmission in suprachiasmatic nucleus neurons. The Journal of neuroscience : the official journal of the Society for Neuroscience *27*, 11748-11757.
21. Colwell, C.S. (2011). Linking neural activity and molecular oscillations in the SCN. Nature reviews. Neuroscience *12*, 553-569.
22. Shigeyoshi, Y., Taguchi, K., Yamamoto, S., Takekida, S., Yan, L., Tei, H., Moriya, T., Shibata, S., Loros, J.J., Dunlap, J.C., et al. (1997). Light-induced resetting of a mammalian circadian clock is associated with rapid induction of the mPer1 transcript. Cell *91*, 1043-1053.
23. Travnickova-Bendova, Z., Cermakian, N., Reppert, S.M., and Sassone-Corsi, P. (2002). Bimodal regulation of mPeriod promoters by CREB-dependent signaling and CLOCK/BMAL1 activity. Proceedings of the National Academy of Sciences of the United States of America *99*, 7728-7733.
24. Kornhauser, J.M., Mayo, K.E., and Takahashi, J.S. (1996). Light, immediate-early genes, and circadian rhythms. Behavior genetics *26*, 221-240.
25. Albrecht, U. (2012). Timing to perfection: the biology of central and peripheral circadian clocks. Neuron *74*, 246-260.

26. Colwell, C.S., Michel, S., Itri, J., Rodriguez, W., Tam, J., Lelievre, V., Hu, Z., Liu, X., and Waschek, J.A. (2003). Disrupted circadian rhythms in VIP- and PHI-deficient mice. American journal of physiology. Regulatory, integrative and comparative physiology *285*, R939-949.
27. van Diepen, H.C., Ramkisoensing, A., Peirson, S.N., Foster, R.G., and Meijer, J.H. (2013). Irradiance encoding in the suprachiasmatic nuclei by rod and cone photoreceptors. Faseb J.
28. Lucassen, E.A., van Diepen, H.C., Houben, T., Michel, S., Colwell, C.S., and Meijer, J.H. (2012). Role of vasoactive intestinal peptide in seasonal encoding by the suprachiasmatic nucleus clock. The European journal of neuroscience *35*, 1466-1474.
29. Michel, S., Marek, R., Vanderleest, H.T., Vansteensel, M.J., Schwartz, W.J., Colwell, C.S., and Meijer, J.H. (2013). Mechanism of bilateral communication in the suprachiasmatic nucleus. The European journal of neuroscience *37*, 964-971.
30. Piggins, H.D., Antle, M.C., and Rusak, B. (1995). Neuropeptides phase shift the mammalian circadian pacemaker. The Journal of neuroscience : the official journal of the Society for Neuroscience *15*, 5612-5622.
31. Albers, H.E., Liou, S.Y., Stopa, E.G., and Zoeller, R.T. (1991). Interaction of colocalized neuropeptides: functional significance in the circadian timing system. The Journal of neuroscience : the official journal of the Society for Neuroscience *11*, 846-851.
32. Nielsen, H.S., Hannibal, J., and Fahrenkrug, J. (2002). Vasoactive intestinal polypeptide induces per1 and per2 gene expression in the rat suprachiasmatic nucleus late at night. The European journal of neuroscience *15*, 570-574.
33. Watanabe, K., Vanecek, J., and Yamaoka, S. (2000). In vitro entrainment of the circadian rhythm of vasopressin-releasing cells in suprachiasmatic nucleus by vasoactive intestinal polypeptide. Brain research *877*, 361-366.
34. Reed, H.E., Meyer-Spasche, A., Cutler, D.J., Coen, C.W., and Piggins, H.D. (2001). Vasoactive intestinal polypeptide (VIP) phase-shifts the rat suprachiasmatic nucleus clock in vitro. The European journal of neuroscience *13*, 839-843.
35. Aton, S.J., Colwell, C.S., Harmar, A.J., Waschek, J., and Herzog, E.D. (2005). Vasoactive intestinal polypeptide mediates circadian rhythmicity and synchrony in mammalian clock neurons. Nature neuroscience *8*, 476-483.
36. Ciarleglio, C.M., Gamble, K.L., Axley, J.C., Strauss, B.R., Cohen, J.Y., Colwell, C.S., and McMahon, D.G. (2009). Population encoding by circadian clock neurons organizes circadian behavior. The Journal of neuroscience : the official journal of the Society for Neuroscience *29*, 1670-1676.
37. Harmar, A.J., Marston, H.M., Shen, S., Spratt, C., West, K.M., Sheward, W.J., Morrison, C.F., Dorin, J.R., Piggins, H.D., Reubi, J.C., et al. (2002). The VPAC(2) receptor is essential for circadian function in the mouse suprachiasmatic nuclei. Cell *109*, 497-508.
38. Nakamura, T.J., Fujimura, K., Ebihara, S., and Shinohara, K. (2004). Light response of the neuronal firing activity in the suprachiasmatic nucleus of mice. Neuroscience letters *371*, 244-248.
39. Drouyer, E., Rieux, C., Hut, R.A., and Cooper, H.M. (2007). Responses of suprachiasmatic nucleus neurons to light and dark adaptation: relative contributions of melanopsin and rod-cone inputs. The Journal of neuroscience : the official journal of the Society for Neuroscience *27*, 9623-9631.
40. Brown, T.M., Wynne, J., Piggins, H.D., and Lucas, R.J. (2011). Multiple hypothalamic cell populations encoding distinct visual information. The Journal of physiology *589*, 1173-1194.

41. Ding, J.M., Chen, D., Weber, E.T., Faiman, L.E., Rea, M.A., and Gillette, M.U. (1994). Resetting the biological clock: mediation of nocturnal circadian shifts by glutamate and NO. Science *266*, 1713-1717.
42. Colwell, C.S., Ralph, M.R., and Menaker, M. (1990). Do NMDA receptors mediate the effects of light on circadian behavior? Brain research *523*, 117-120.
43. Colwell, C.S. (2001). NMDA-evoked calcium transients and currents in the suprachiasmatic nucleus: gating by the circadian system. The European journal of neuroscience *13*, 1420-1428.
44. Pennartz, C.M., Hamstra, R., and Geurtsen, A.M. (2001). Enhanced NMDA receptor activity in retinal inputs to the rat suprachiasmatic nucleus during the subjective night. The Journal of physiology *532*, 181-194.
45. Wang, L.M., Schroeder, A., Loh, D., Smith, D., Lin, K., Han, J.H., Michel, S., Hummer, D.L., Ehlen, J.C., Albers, H.E., et al. (2008). Role for the NR2B subunit of the N-methyl-D-aspartate receptor in mediating light input to the circadian system. The European journal of neuroscience *27*, 1771-1779.
46. Kim, D.Y., Choi, H.J., Kim, J.S., Kim, Y.S., Jeong, D.U., Shin, H.C., Kim, M.J., Han, H.C., Hong, S.K., and Kim, Y.I. (2005). Voltage-gated calcium channels play crucial roles in the glutamate-induced phase shifts of the rat suprachiasmatic circadian clock. The European journal of neuroscience *21*, 1215-1222.
47. Brancaccio, M., Enoki, R., Mazuski, C.N., Jones, J., Evans, J.A., and Azzi, A. (2014). Network-mediated encoding of circadian time: the suprachiasmatic nucleus (SCN) from genes to neurons to circuits, and back. The Journal of neuroscience : the official journal of the Society for Neuroscience *34*, 15192-15199.
48. Pauls, S., Foley, N.C., Foley, D.K., LeSauter, J., Hastings, M.H., Maywood, E.S., and Silver, R. (2014). Differential contributions of intra-cellular and inter-cellular mechanisms to the spatial and temporal architecture of the suprachiasmatic nucleus circadian circuitry in wild-type, cryptochrome-null and vasoactive intestinal peptide receptor 2-null mutant mice. The European journal of neuroscience *40*, 2528-2540.
49. Kornhauser, J.M., Ginty, D.D., Greenberg, M.E., Mayo, K.E., and Takahashi, J.S. (1996). Light entrainment and activation of signal transduction pathways in the SCN. Progress in brain research *111*, 133-146.
50. Shearman, L.P., Zylka, M.J., Weaver, D.R., Kolakowski, L.F., Jr., and Reppert, S.M. (1997). Two period homologs: circadian expression and photic regulation in the suprachiasmatic nuclei. Neuron *19*, 1261-1269.
51. Gau, D., Lemberger, T., von Gall, C., Kretz, O., Le Minh, N., Gass, P., Schmid, W., Schibler, U., Korf, H.W., and Schutz, G. (2002). Phosphorylation of CREB Ser142 regulates light-induced phase shifts of the circadian clock. Neuron *34*, 245-253.
52. Dragich, J.M., Loh, D.H., Wang, L.M., Vosko, A.M., Kudo, T., Nakamura, T.J., Odom, I.H., Tateyama, S., Hagopian, A., Waschek, J.A., et al. (2010). The role of the neuropeptides PACAP and VIP in the photic regulation of gene expression in the suprachiasmatic nucleus. The European journal of neuroscience *31*, 864-875.
53. Hamada, T., Antle, M.C., and Silver, R. (2004). Temporal and spatial expression patterns of canonical clock genes and clock-controlled genes in the suprachiasmatic nucleus. The European journal of neuroscience *19*, 1741-1748.
54. Han, S., Yu, F.H., Schwartz, M.D., Linton, J.D., Bosma, M.M., Hurley, J.B., Catterall, W.A., and de la Iglesia, H.O. (2012). Na(V)1.1 channels are critical for intercellular communication in the suprachiasmatic nucleus and for normal circadian rhythms. Proceedings of the National Academy of Sciences of the United States of America *109*, E368-377.

55. Dardente, H., Poirel, V.J., Klosen, P., Pevet, P., and Masson-Pevet, M. (2002). Per and neuropeptide expression in the rat suprachiasmatic nuclei: compartmentalization and differential cellular induction by light. Brain research *958*, 261-271.
56. Guido, M.E., de Guido, L., Goguen, D., Robertson, H.A., and Rusak, B. (1999). Differential effects of glutamatergic blockade on circadian and photic regulation of gene expression in the hamster suprachiasmatic nucleus. Brain research. Molecular brain research *67*, 247-257.
57. Karatsoreos, I.N., Yan, L., LeSauter, J., and Silver, R. (2004). Phenotype matters: identification of light-responsive cells in the mouse suprachiasmatic nucleus. The Journal of neuroscience : the official journal of the Society for Neuroscience *24*, 68-75.
58. Kuhlman, S.J., Silver, R., Le Sauter, J., Bult-Ito, A., and McMahon, D.G. (2003). Phase resetting light pulses induce Per1 and persistent spike activity in a subpopulation of biological clock neurons. The Journal of neuroscience : the official journal of the Society for Neuroscience *23*, 1441-1450.
59. Schwartz, W.J., Carpino, A., Jr., de la Iglesia, H.O., Baler, R., Klein, D.C., Nakabeppu, Y., and Aronin, N. (2000). Differential regulation of fos family genes in the ventrolateral and dorsomedial subdivisions of the rat suprachiasmatic nucleus. Neuroscience *98*, 535-547.
60. Yan, L., Takekida, S., Shigeyoshi, Y., and Okamura, H. (1999). Per1 and Per2 gene expression in the rat suprachiasmatic nucleus: circadian profile and the compartment-specific response to light. Neuroscience *94*, 141-150.
61. Nakamura, W., Yamazaki, S., Takasu, N.N., Mishima, K., and Block, G.D. (2005). Differential response of Period 1 expression within the suprachiasmatic nucleus. The Journal of neuroscience : the official journal of the Society for Neuroscience *25*, 5481-5487.
62. Yan, L., and Okamura, H. (2002). Gradients in the circadian expression of Per1 and Per2 genes in the rat suprachiasmatic nucleus. The European journal of neuroscience *15*, 1153-1162.
63. An, S., Tsai, C., Ronecker, J., Bayly, A., and Herzog, E.D. (2012). Spatiotemporal distribution of vasoactive intestinal polypeptide receptor 2 in mouse suprachiasmatic nucleus. The Journal of comparative neurology *520*, 2730-2741.
64. Gamble, K.L., Allen, G.C., Zhou, T., and McMahon, D.G. (2007). Gastrin-releasing peptide mediates light-like resetting of the suprachiasmatic nucleus circadian pacemaker through cAMP response element-binding protein and Per1 activation. J Neurosci *27*, 12078-12087.
65. Gamble, K.L., Kudo, T., Colwell, C.S., and McMahon, D.G. (2011). Gastrin-releasing peptide modulates fast delayed rectifier potassium current in Per1-expressing SCN neurons. J Biol Rhythms *26*, 99-106.
66. LeSauter, J., Silver, R., Cloues, R., and Witkovsky, P. (2011). Light exposure induces short- and long-term changes in the excitability of retinorecipient neurons in suprachiasmatic nucleus. J Neurophysiol *106*, 576-588.
67. Jeftinija, S., Murase, K., Nedeljkov, V., and Randic, M. (1982). Vasoactive intestinal polypeptide excites mammalian dorsal horn neurons both in vivo and in vitro. Brain Res *243*, 158-164.
68. Pawelzik, H., Dodt, H.U., and Zieglgansberger, W. (1992). Actions of vasoactive intestinal polypeptide (VIP) on neocortical neurons of the rat in vitro. Neurosci Lett *147*, 167-170.
69. Lee, S.H., and Cox, C.L. (2006). Excitatory actions of vasoactive intestinal peptide on mouse thalamocortical neurons are mediated by VPAC2 receptors. J Neurophysiol *96*, 858-871.
70. Hermes, M.L., Kolaj, M., Doroshenko, P., Coderre, E., and Renaud, L.P. (2009). Effects of VPAC2 receptor activation on membrane excitability and GABAergic transmission in

subparaventricular zone neurons targeted by suprachiasmatic nucleus. J Neurophysiol *102*, 1834-1842.

71. Pakhotin, P., Harmar, A.J., Verkhratsky, A., and Piggins, H. (2006). VIP receptors control excitability of suprachiasmatic nuclei neurones. Pflugers Archiv : European journal of physiology *452*, 7-15.
72. Berson, D.M., Dunn, F.A., and Takao, M. (2002). Phototransduction by retinal ganglion cells that set the circadian clock. Science *295*, 1070-1073.
73. Tu, D.C., Zhang, D., Demas, J., Slutsky, E.B., Provencio, I., Holy, T.E., and Van Gelder, R.N. (2005). Physiologic diversity and development of intrinsically photosensitive retinal ganglion cells. Neuron *48*, 987-999.
74. Warren, E.J., Allen, C.N., Brown, R.L., and Robinson, D.W. (2003). Intrinsic light responses of retinal ganglion cells projecting to the circadian system. The European journal of neuroscience *17*, 1727-1735.
75. McMahon, D.G., and Block, G.D. (1987). The Bulla ocular circadian pacemaker. I. Pacemaker neuron membrane potential controls phase through a calcium-dependent mechanism. Journal of comparative physiology. A, Sensory, neural, and behavioral physiology *161*, 335-346.
76. Hughes, A.T., Fahey, B., Cutler, D.J., Coogan, A.N., and Piggins, H.D. (2004). Aberrant gating of photic input to the suprachiasmatic circadian pacemaker of mice lacking the VPAC2 receptor. The Journal of neuroscience : the official journal of the Society for Neuroscience *24*, 3522-3526.
77. Itri, J., and Colwell, C.S. (2003). Regulation of inhibitory synaptic transmission by vasoactive intestinal peptide (VIP) in the mouse suprachiasmatic nucleus. Journal of neurophysiology *90*, 1589-1597.
78. Michel, S., Itri, J., and Colwell, C.S. (2002). Excitatory mechanisms in the suprachiasmatic nucleus: the role of AMPA/KA glutamate receptors. Journal of neurophysiology *88*, 817-828.

SUPPLEMENTARY MATERIALS

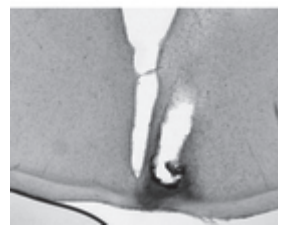

S. Figure 1. An example of a coronal slice of the mouse brain with the SCN right above the optic chiasm at the base of the hypothalamus (left panel). The location of the electrode can be verified by the blue spot, which is marked using an electrolytic current (right panel).

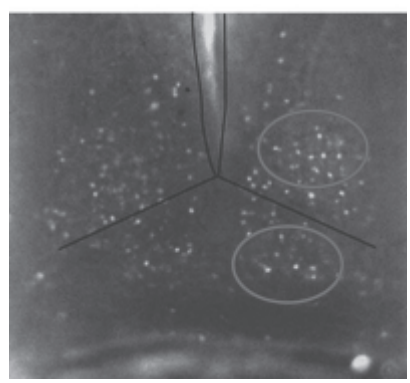

S. Figure 2. Image of Fura2-labeled SCN slice. The ventral tip of the 3rd ventricle serves as a reference point for our physiological or calcium measurements. Cells dorsal to the tip are considered "dorsal" SCN while cells ventral to the tip are considered "ventral" SCN. There is an area in the middle from which we do not record as it would be difficult to place the cells into these categories. In previous studies, we have used biocytin-fills to confirm that our visually placed cells indeed are localized into the ventral or dorsal regions [77, 78]. Thus, we believe that the data indicates that we can differentiate dorsal vs. ventral cell populations. This technique does not allow us to differentiate core vs. shell which is defined by peptide co-expression.

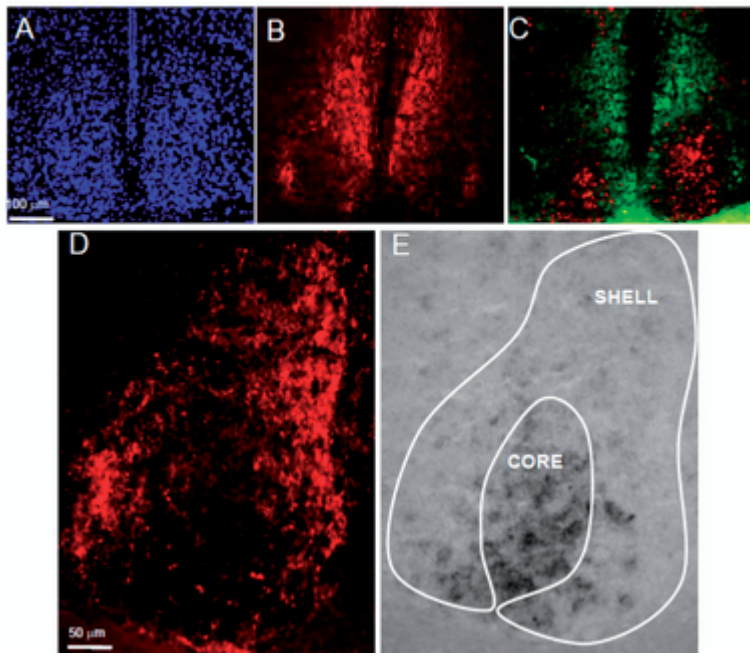

S. Figure 3. Different SCN markers were used to create core and shell templates to overlay on alternately stained *Per1*-expressing SCN photomicrographs. (A) DAPI traditionally localizes the SCN and its landmarks based on dense cell body staining around the third ventricle, just above the optic chiasm. (B) Arginine-vasopressin (AVP) is used to delineate SCN boundaries as well as demarcate the SCN shell. (C) Double labeling for AVP (green) and androgen receptor (AR) (red), confirms that this region is appropriate labeled as core. (D and E) Templates were drawn around the AVP+ SCN area to define core and shell, and templates were overlaid onto alternate sections (20µM) to apply to quantification of *Per1* expression across SCN regions.

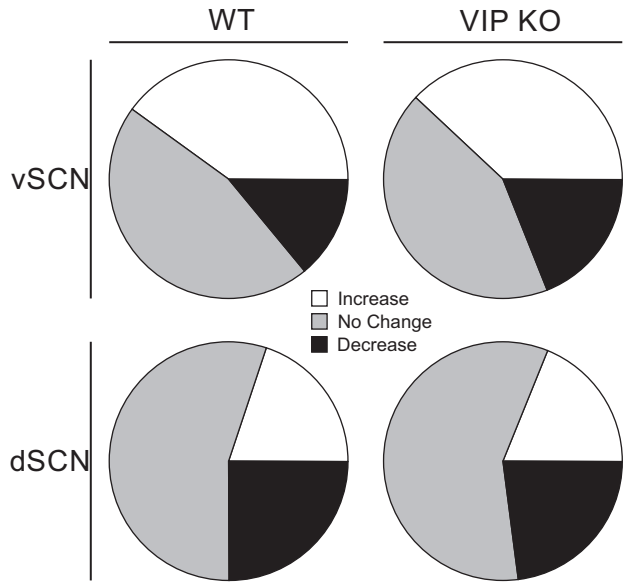

S. Figure 4. Distribution of Ca^{2+} responses as a result of RHT stimulation. SCN neurons responded to RHT stimulation with either increases (white), decreases (black), or no change (grey) in Ca^{2+} levels. The distribution of the response types was dependent on the region, but did not change between genotypes.